Endophytic pyrroloquinoline quinone enhances banana growth and immunity against *Fusarium* wilt for plant-microbe mutualisms

Running Title: PQQ coordinates plant growth and immunity

Shih-Hsun Walter Hung[1,2,3,4], Man-Yun Yu[1], Chia-Ho Liu[1], Tsai-Ching Huang[1], Jian-Hau Peng[5,6], Nai-Yun Jang[1], Chih-Horng Kuo[2,5,6,7], Ying-Ning Ho[8,9,10], En-Pei Isabel Chiang[3,4,5,6,11], Hau-Hsuan Hwang[1,3,4,5,6], and Chieh-Chen Huang[1,3,4,5,6]*

[1] Department of Life Sciences, National Chung Hsing University, Taichung 402202, Taiwan; [2] Institute of Plant and Microbial Biology, Academia Sinica, Taipei 115201, Taiwan; [3] Advanced Plant and Food Crop Biotechnology Center, National Chung Hsing University, Taichung 402202, Taiwan; [4] Innovation and Development Centre of Sustainable Agriculture, National Chung Hsing University, Taichung 402202, Taiwan; [5] PhD Program in Microbial Genomics, National Chung Hsing University, Taichung 402202, Taiwan; [6] PhD Program in Microbial Genomics, Academia Sinica, Taipei 115201, Taiwan; [7] Biotechnology Center, National Chung Hsing University, Taichung 402202, Taiwan; [8] Institute of Marine Biology, College of Life Science, National Taiwan Ocean University, Keelung 202301, Taiwan; [9] Center of Excellence for the Oceans, National Taiwan Ocean University, Keelung 202301, Taiwan; [10] Taiwan Ocean Genome Center, National Taiwan Ocean University, Keelung 202301, Taiwan; [11] Department of Food Science and Biotechnology, National Chung Hsing University, Taichung 402202, Taiwan

***Correspondence**: Chieh-Chen Huang; cchuang@dragon.nchu.edu.tw

ORCID SHW Hung, 0000-0002-8749-5653; CH Liu, 0000-0001-9166-3966; TC Huang, 0000-0002-3410-2051; JH Peng, 0000-0001-6052-8606; CH Kuo, 0000-0002-2857-0529; YN Ho, 0000-0003-0943-1416; EPI Chiang, 0000-0002-0158-0962; HH Hwang, 0000-0001-9132-0242; CC Huang, 0000-0002-3739-6315.

Keywords: endophyte, symbiosis, pyrroloquinoline quinone (PQQ), *Fusarium* wilt of banana, molecular plant-microbe interactions (MPMI)

Abstract

Fusarium wilt has a substantial impact on global banana production, posing a threat to food security worldwide. However, breeding new *Fusarium*-resistant cultivars is difficult and time-consuming. Alternatively, endophytic biostimulants that could combat such pervasive plant diseases provide possible novel solutions. Our prior research demonstrated that a pyrroloquinoline quinone (PQQ)–producing endophytic bacterium, *Burkholderia seminalis* 869T2, can enhance the growth of various plant species and protect bananas from *Fusarium* wilt in the field. PQQ is a peptide-derived redox cofactor known to stimulate mitochondrial biogenesis and metabolism in animals, but its molecular roles, especially in plants, remain to be elucidated. In this study, multi-omics approaches were employed to explore the potential mechanisms through which PQQ influences banana plants. The result of *in situ* imaging mass spectrometry revealed that the endophytic metabolite PQQ does not function through direct antagonism against *Fusarium*. The follow-up transcriptomic profiling shows it could regulate plant respiration, TCA cycle, oxidative phosphorylation, NAD/NADP–dependent dehydrogenases, MAPK signalling, and various phytohormone signalling pathways. Furthermore, PQQ appeared to trigger plant systemic immunity, thereby enhancing plant health and resistance to biotic stress. Beyond that, the complete genome of 869T2 was determined for follow-up comparative genomics analyses, revealing its genetic contexts, potential evolutionary events of PQQ operons among the *Burkholderia* species, and the absence of human virulence-facilitating genes within those PQQ-producing agricultural isolates. In summary, this study facilitates our understanding of PQQ in plant-microbe mutualisms and provides scientific evidence for its future application in agriculture.

Significance Statement

Fusarium wilt is caused by *Fusarium oxysporum* f. sp. *cubense* tropical race 4 (*Foc* TR4), a notorious soil-borne pathogen that attacks bananas' vascular system, which critically threatens global banana production and food security. A potential PQQ-producing endophytic strain has been confirmed to protect bananas through *in planta* biocontrol, reducing the morbidity of Banana *Fusarium* Wilt (BFW) disease in the field and promoting the growth of banana plants simultaneously. Our results revealed that the endophytic metabolite PQQ does not function through direct antagonism but triggers plant systemic immunity and coordinates energetic metabolisms, thereby improving the overall health of host plants and enhancing their resistance against *Fusarium* wilt.

67 **Main Text**

68 ## Introduction

69 Pyrroloquinoline quinone (PQQ), also known as methoxatin, was initially identified as
70 a unique quinone-like cofactor that partners with bacterial glucose and alcohol
71 dehydrogenases, as reported in early studies (1, 2). Subsequent research uncovered a
72 variety of PQQ-dependent dehydrogenases in prokaryotes, which process substances like
73 methanol, alcohol, aldehydes, and sugars (3–5). Initially thought to be exclusive to
74 prokaryotes, PQQ was later discovered in eukaryotic organisms, including animals and
75 plants (6). Serving as a redox cofactor for several dehydrogenases, PQQ is integral to vital
76 metabolic processes across different life forms of kingdoms (7, 8). Its diverse benefits, both
77 in vivo and in vitro, have been demonstrated in numerous studies focusing on microbes and
78 animals. For example, PQQ acts as a powerful antioxidant by neutralizing reactive oxygen
79 species (ROS) (9), it helps maintain the balance of nicotinamide adenine dinucleotide levels
80 (9), and it stimulates the creation of mitochondria (10, 11), thereby enhancing energy-
81 related metabolisms such as oxidative phosphorylation and ATP production (12, 13).
82 However, the impact of PQQ on plant molecular biology is not well understood. Recent
83 findings suggest that PQQ can eliminate ROS in plants similarly to its function in animals
84 (14). Additionally, PQQ appears to enhance the glucose dehydrogenase activity and
85 phosphate-solubilizing abilities of plant growth-promoting bacteria (15–19), and it may also
86 bolster the antifungal defence of plants by supporting plant-associated microbes (20, 21).
87 Nevertheless, the precise molecular mechanisms underlying these effects are still to be
88 elucidated.

89 On the other hand, *Fusarium oxysporum* f. sp. *cubense* tropical race 4 (*Foc* TR4) is a
90 notorious soil-borne pathogen that attacks the vascular system of bananas, critically
91 threatening banana production and having severe consequences on global food security
92 and the livelihoods of around 400 million people (22, 23). The most effective approach to
93 combat this highly destructive and aggressive fungus is to prevent its initial spread, as it can
94 cause complete yield loss once established in a field (24). Currently, over 80% of global
95 banana production relies on Foc TR4-susceptible germplasm (25). Given the challenge of
96 breeding new varieties or cultivars that are both suitable for the value chain and resistant to
97 disease, new technologies for accelerating precise breeding and biological agents for in-
98 field protection are urgently needed. Some plant symbionts have been reported to protect
99 banana plants against *Foc* TR4 (26–29), and some microbial metabolites function as
100 biostimulants, resulting in plant disease protection through exogenous supplementation (30,
101 31).

102 Our previous works isolated and characterised a potential PQQ-producing
103 endophyte, *Burkholderia seminalis* 869T2, which confers strong resistance to *Fusarium*
104 *oxysporum* f. sp. *cubense* tropical race 4 (Foc TR4) (28, 32). This endophytic strain has
105 been confirmed to protect bananas in field tests through *in planta* biocontrol, reducing the

106 morbidity of Banana *Fusarium* Wilt disease from 24.5% to 3.4% while also promoting the
107 growth of banana plants (28). Besides those positive effects brought on bananas, strain
108 869T2 and its metabolites have been established as plant-beneficial or stress-resilient
109 endophytic biostimulants that promote the growth of various crops, including *Brassica*,
110 *Lactuca*, *Amaranthus*, *Capsicum*, and *Abelmoschus* (33, 34). The strain has also been
111 established as a versatile endophytic biostimulant for leafy vegetables. It significantly
112 promotes plant growth and enhances crop quality by increasing harvested head weight, size
113 and nutrient composition. Additionally, a two-week acceleration in harvest time and 50%
114 savings on fertilising costs result in reducing costs and increasing product value
115 simultaneously, which provides a model for in-field endophytic biostimulants-assisted smart
116 agricultural management for lettuce production (34). On the other hand, the bioremediation
117 availability of 869T2 for the degradation of persistent organic pollutants (POPs), such as
118 dioxins, under an aerobic environment through 2-haloacid dehalogenase has also been
119 demonstrated (35). These results emphasize the importance of endophytic bacteria,
120 warranting further investigation due to their enigmatic symbiotic relationships with hosts and
121 potential applications in the agro-industry.

122 In this study, our goal was to better understand the molecular mechanisms of
123 endophytic PQQ *in planta*, particularly in the context of plant-microbe mutualistic symbiosis
124 and the defence against pathogens. Our result revealed that endophytic PQQ has no direct
125 antagonism activity to inhibit the growth of *Fusarium* species. Instead, it promotes the
126 overall health of host plants by triggering plant immunity through the modulation of multiple
127 phytohormones and MAPK signalling pathways. Additionally, it coordinates their energetic
128 metabolisms, including the TCA cycle, oxidative phosphorylation, and the biosynthesis and
129 activity of NAD/NADP-dependent enzymes. Meanwhile, the results of comparative
130 genomics shed light on the evolution of the pqq operon and other genetic contents, thus
131 offering clues about the co-evolution and mutualistic relationships among those plant-
132 associated bacteria with their hosts.

133 ## Results

134 ### Species reclassification of strain 869T2 to *Burkholderia seminalis*

135 Strain 869T2 was initially identified as *Burkholderia cenocepacia* with its draft
136 genome sequence (32). However, updated analysis of molecular phylogeny and gene
137 content indicated that this strain is more similar to *B. seminalis* (36). Therefore, complete
138 genome sequencing and comparative analyses were performed in this work to determine its
139 species assignment.

140 For hybrid *de novo* assembly, 2 x 3,178,899 (~1.9 Gb) of Illumina and 46,153 (~0.5
141 Gb) of untrimmed ONT raw reads were generated, which provided ~238- and ~65-fold
142 coverages for this genome, respectively. The assembly result indicated that 869T2 has
143 three circular chromosomes totalling 8,022,336 bp and an average GC content of 67.03%.
144 The comparison against a reference Burkholderiales dataset identified 687 complete
145 BUSCOs (99.9%), one fragmented BUSCOs (0.1%), and no missing BUSCOs within this
146 genome assembly, supporting that the genome assembly is complete. The annotation
147 showed that this genome contains six complete sets of rRNA genes, 67 tRNA genes, four
148 ncRNAs, 7,090 protein-coding genes and 112 pseudogenes (Table S1).

149 For the species assignment, the newly generated complete genome sequence was
150 utilised for comparative analysis with key representatives of *B. seminalis* and *B.*
151 *cenocepacia* (Table S2) based on genome-wide average nucleotide identity (ANI) and core-
152 genome phylogeny. The result showed that 869T2 shares ~93-95% of its genome with other
153 *B. seminalis* strains and has > 99% ANI (Fig. 1A). In contrast, 869T2 shares only ~79-82%
154 of its genome and has < 93% ANI when compared to *B. cenocepacia* strains. Additionally,
155 3,018 single-copy genes shared by all strains were identified and used to produce a
156 concatenated alignment containing 987,390 aligned amino acid sites for maximum
157 likelihood phylogeny inference (Fig. 1A). Based on 1,000 resamplings, the resulting tree had
158 100% bootstrap support value for all internal branches and 869T2 is a member of the *B.*
159 *seminalis* clade. Based on these results, strain 869T2 can be confidently re-classified as a
160 member of *B. seminalis*.

161

162 ### Gene content analysis between *B. cenocepacia* and *B. seminalis*

163 For more in-depth analysis, the gene content of representative *B. seminalis* and *B.*
164 *cenocepacia* strains was compared. Specifically, genes known to be related to
165 environmental adaptation and molecular plant-microbe interactions (MPMI) were the main
166 targets (Fig. 1B and Table S3). A distinct differentiation was observed for genes encode for
167 nitrile hydratase cluster (*nthAB*), phenylacetaldoxime dehydratase (*oxd*), galacturonate
168 metabolism (*uxa*), indoleacetic acid (IAA) biosynthesis (*iaaHM*), and pyrrolnitrin biosynthesis
169 (*prnABCD*); these genes were conserved among *B. seminalis* strains but mostly absent

170 among *B. cenocepacia* strains (Fig. 1B). Additionally, *B. seminalis* strains mostly have two
171 copies of genes for feruloyl esterase (*faeB*) and ACC deaminase (*acdS*). On the other hand,
172 genes involved in virulence to human (*esmR*, *amiI*, *cciI*, *cciR*, and *opcI*) (37) were found
173 only in *B. cenocepacia* strains, but absent in all of the *B. seminalis* strains examined (Fig.
174 1B), which mitigate the risk of using *B. seminalis* strains such as 869T2 for agricultural
175 application. Finally, the *pqq* operon, encoding essential genes responsible for the
176 biosynthesis of PQQ, is conserved in most of the strains examined.

177

178 **PQQ cannot antagonise *Fusarium in vitro***

179 Given that 869T2 has various plant-growth-promoting (PGP) traits and abundant
180 MPMI-related genetic contents, we used the ultra-high performance liquid chromatography-
181 tandem mass spectrometry (UHPLC-MS/MS) technique to determine its metabolome and
182 target the specific chemicals responsible for the PGP or pathogen resistance potential. The
183 results showed that 869T2 produces multiple phytohormones, including auxin, cytokinin,
184 gibberellic acid, ethylene and salicylic acid, as well as the corresponding regulatory factors
185 were confirmed (Table S4). Besides, 31 cyclic dipeptides (CDPs) were identified; some
186 CDPs were found as antimicrobial substances and antibiotics (Table S5). Furthermore,
187 along with a biosynthesis operon of pyrrolnitrin, an antibiotic that suppresses *Fusarium*
188 species (38), four of its antifungal derivates: iso-, oxy- and fluoro-pyrrolnitrin and 3-chloro-4-
189 (2-nitrophenyl)-1H-pyrrole were also detected. These results suggested that 869T2 could
190 inhibit the growth of fungi, *e.g.*, *Foc* TR4, via specific antifungal compounds.

191 A follow-up *in situ* metabolic investigation using the matrix-assisted laser desorption
192 ionization-time of flight (MALDI-TOF) imaging mass spectrometry (IMS) technique also
193 confirmed that 869T2 produced pyrrolnitrin and its derivatives, oxypyrrolnitrin or 3-Chloro-4-
194 (3-chloro-4-fluoro-2-nitrophenyl) pyrrole, to inhibit the growth *Foc* TR4 *in vitro* (Fig. 2A).
195 Strikingly, the signal of endophytic biostimulants PQQ was found and was only detected
196 when incubating without *Foc* TR4 (Fig. 2B); the endophytic PQQ production was further
197 confirmed through gas chromatography-mass spectrometry (GC-MS) by comparing to the
198 synthetic PQQ standard (>98% purity) (Fig. S1). Previous studies suggested mutagenesis
199 on *pqqC* and *pqqE*, essential genes for PQQ biosynthesis, affects the bacterial antimicrobial
200 activity *in vitro* or *in planta* (20, 21, 39). However, our imaging mass results suggested that
201 the production of PQQ seems irrelevant to the *Fusarium* inhibition. To explain this
202 paradoxical relationship, an antagonism assay was performed using levels of synthetic PQQ
203 standards as treatments and *B. seminalis* 869T2 as a control. The results showed that PQQ
204 has no positive effects on inhibiting the growth of *Foc* TR4 but improves it instead (Fig. 2C).
205 Based on this evidence, we raise another possibility that PQQ may induce plant immunity,
206 resulting in antimicrobial activity in plants. To examine our hypothesis, synthetic PQQ was
207 exogenously supplemented to banana plantlets, and the morbidity to *Fusarium* wilt and

208 plant transcriptomics were investigated to unveil the obscure molecular mechanisms among
209 them.

210

211 **Exogenous supplementation of PQQ induces the growth and development of banana**
212 **plants**

213 Firstly, 5 nM, 50 nM, 100 nM and 1000 nM PQQ, hereinafter referred to as P05, P50,
214 P100 and P1000, respectively, were examined on tissue culture banana plantlets; about
215 twenty biological replications were set for each treatment. At 48 days after treatment (DPT),
216 the results showed that exogenous PQQ supplementation contributes to the differentiation
217 of both shoot and root (Fig. 3A-C). Among them, by estimating using the developmental
218 indicator N_{50}, defined as the shoot/root length of the shortest organ at 50% of the total
219 shoot/root length, P100 seems an ideal dosage for triggering plant leaf and root
220 development. For root development: (a) P100 had three plantlets without visible root
221 development (CK had seven); (b) the root N_{50} of P100 was at level 7-8 (CK was at level 3-
222 4); (c) the maximum root order of P100 was at level >9 (CK was at level 5-6) (Fig. 3B). For
223 leaf development: (a) P100 had four plantlets without visible leaf development (CK had the
224 same); (b) the leaf N_{50} of P100 was at level 3 (CK was at level 2); (c) the maximum leaf
225 order of P100 was at level 5 (CK was at level 3) (Fig. 3C).

226 Besides, significantly more root and leaf numbers were both observed in P50 and
227 P100 (Fig. 3D,E); all treatments significantly elongated the root length (Fig. 3F) while only
228 P100 promoted the plant height compared to the CK with statistical significance (Fig. 3G).
229 These positive effects on plant growth and development were found to remain after the
230 bananas were transplanted to soil pots at least until 137 DPT (Fig. S2). Given that P1000
231 did not constantly improve plant growth and even contributed less than P100, we
232 hypothesise that a high dosage of PQQ supplementation may inhibit plant growth.
233 Therefore, additional experimental batches, including P100, P1000, and P2000 (2000 nM
234 PQQ), were performed to delineate the boundary of its working concentration. The
235 phenotypic results together suggested that the supplementation concentration over 100 nM
236 had no significant positive effects and, in some cases, harmed the plants instead (Fig. S3).
237 For instance, the fresh weight and plant height of the 1000 nM treatments decreased from
238 0.66 ± 0.06 g to 0.59 ± 0.08 g (Fig. S3B) and from 2.46 ± 0.13 cm to 2.25 ± 0.12 cm (Fig.
239 S3E), respectively. Accordingly, PQQ concentrations over 100 nM were considered to affect
240 plants negatively and were excluded from the follow-up experiments.

241

242 **Transcriptomic landscape of banana plants in response to PQQ**

243 To unveil the molecular roles of PQQ in plants, total RNA was extracted from the CK
244 and 100 nM PQQ treatments, respectively, and used for the following transcriptomic

245 analysis. Totally ~6.5 Gb raw reads were obtained from each sample through the Illumina
246 Hiseq4000 2 x 150 bp sequencing. After mapping the resultants to the banana reference
247 genome (NCBI TaxID: 214687), a total of 25,070 variables were identified (Fig. 4A). Among
248 them, 1,181 and 592 differentially expressed genes (DEGs) were identified through gene
249 ontology (GO) enrichment analysis ($p < 0.05$ and FC >2) and Kyoto Encyclopedia of Genes
250 and Genomes (KEGG) analysis ($p < 0.05$ and FC >1), respectively (Fig. 4B,C).

251 The GO analysis showed that molecular function terms like regulations in heme
252 binding, peroxidase activity, ATPase activity, etc. were found to be enriched regulated.
253 Several DEGs were identified as involved within the chloroplast and mitochondria-related
254 metabolisms within biological processes and cell components terms (Fig. 4B). For KEGG,
255 the DEGs were assigned to 92 pathways, and the 11 pathways, including phenylpropanoid
256 biosynthesis, plant hormone signal transduction, ABC transporters, MAPK signalling
257 pathway – plant, plant-pathogen interaction, etc., were further targeted as they were
258 identified as enriched regulated from both down- and up-regulated (Fig. 4C). The detailed
259 profiles of GO and KEGG analyses were provided in supporting information (Tables S6,S7).
260 Besides, the DEGs were accessed to 11 metabolic pathways or enzymatic genes for further
261 analysis based on our enrichment analysis and previous studies to explore the molecular
262 roles participating within plant physiology (Figs. 4D,S4-S19). Considering the transmission
263 of PQQ across the host and microbe, the ABC transporters ABCB1 and ABCG2/PDR5,
264 which are capable of transporting small molecules, were identified as being regulated with
265 statistical significance (Figs. 4D, S4). Echoing previous works that showed that PQQ has
266 reactive oxygen species (ROS) scavenging and stress-resilience availabilities, 16 and 10
267 genes of glutathione and peroxisome metabolisms were found to be differentially regulated,
268 respectively (Figs. 4D,S5,S6).

269 Interestingly, abundant genes responsible for plant respiration and energic
270 metabolisms were found mainly mediated: genes encode essential proteins for the TCA
271 cycle (*e.g.*, citrate synthase, aconitase, isocitrate dehydrogenase, α-ketoglutarate
272 dehydrogenase and malate dehydrogenase) (Figs. 4D,S7) and oxidative phosphorylation
273 (*e.g.*, plasma membrane ATPase, V-type proton ATPase, mitochondrial external alternative
274 NAD(P)H-ubiquinone oxidoreductase B2 and cytochrome c) (Figs. 4D,S8). Genes involved
275 in the glycolysis/gluconeogenesis pathway and pyruvate metabolism (*e.g.*, acetyl-CoA
276 synthetase, aldo-keto reductase, dihydrolipoyl dehydrogenase, phosphoenolpyruvate
277 carboxylase, pyruvate kinase, pyruvate phosphate dikinase, etc.) were also been up-
278 regulated (Fig. 4D,S9,S10) (Table S7). These results strengthen the perspectives on the
279 participation of PQQ in intercellular electron transmission and redox reactions in plant cells.
280 We also analysed those enriched regulated NAD/NADP-dependent enzymes and
281 dehydrogenase to dig into their coordination (Table S8). Although PQQ was mostly
282 suggested to mediate lactate dehydrogenases in animal and microbial cells, these
283 regulations were not found significantly within plant cells. Instead, its regulations on the
284 other dehydrogenases corresponding to aldehyde, malate, glutamate, isocitrates, etc., while
285 ferredoxin reductases were identified as enrichment with significance (Fig. 4D) (Table S7).

286 This result distinguishes the divergence of molecular roles and functions of PQQ as
287 (NAD/NADP-dependent) dehydrogenase among different life kingdoms.

288 In view of the PGP and anti-*Fusarium* properties of PQQ, the DEGs involved in
289 phenylpropanoid metabolisms, phytohormone biosynthesis and signal transduction, the
290 MAPK signalling pathway, and plant-pathogen interaction were focused. Among them, the
291 phenylpropanoid metabolism for the biosynthesis of structural lignin components, which
292 were essential to the plant cell wall construction and strength and rigidity, were been
293 induced (Fig. S11). The tryptophan metabolism for indole acetate (IAA) and biosynthesis
294 pathways of several chemicals with biotic or abiotic stresses alleviating and with antioxidant
295 activities like lutein and zeaxanthin, carotenoids, dopamine, melatonin and flavonoids were
296 also found induced by PQQ (Fig. S12-S16). For plant hormone signal transduction
297 regulations, auxin and stress-associated pathways were particularly regulated, and
298 pathways for those stress hormones, e.g., ethylene, jasmonic acid, and salicylic acid, were
299 significantly enhanced (Fig. S17). Furthermore, in a total of 23 DEGs of the plant's MAPK
300 signalling and plant-pathogen interaction, metabolisms were also induced, which included
301 various pathogen-associated transcriptional factors, ethylene regulations and pathogenesis-
302 related proteins, suggesting putative immune responses to protecting plants against
303 pathogens could be pre-triggered by the exogenous supplementation of PQQ (Figs.
304 S18,S19).

305

306 **Exogenous supplementation of PQQ boosts the immunity of banana plants**

307 The transcriptomics results confirmed previous findings that mutagenesis of PQQ
308 biosynthesis genes negatively impacts microbial biocontrol ability in plants (20, 21, 39).
309 These results also supported our hypothesis that PQQ coordinates plant growth and
310 immunity to protect the host plant against pathogens. To determine if the antifungal activity
311 observed in tissue culture (Figs. 4A, 5A) persists under soil growing conditions, we
312 transplanted banana plants treated with different concentrations of PQQ into soil pots
313 infected with Foc TR4. We then evaluated four indicators of Panama Disease—leaf
314 yellowing (LY), pseudostem splitting (SS), pseudostem bending (SB), and rhizome dark
315 brown discolouration (RB)—to assess the role of PQQ in protecting plants against *Fusarium*
316 wilt of bananas (Fig. 5B, C). Three months after the *Foc* TR4 infection, the Panama Disease
317 indicators of plants growing in soil conditions were investigated. The unweighted pair group
318 method with arithmetic mean (UPGMA) dendrogram clustering and the principal component
319 analysis (PCA) were performed for an integrative evaluation of the diseasing patterns. The
320 UPGMA results indicated that the LY, RB, and SB diseasing patterns of all PQQ treatments
321 were much closer to the negative control (health plants) than the positive control (diseased
322 plants) (Fig. 5D-F). Alike clustering results were found in P50, P100, and P1000 for the SS
323 diseasing patterns, except for P05 (Fig. 5G).

A follow-up PCA suggested a similar result to the UPGMA that the PQQ treatments, especially P50 and P100, help to protect bananas against *Foc* TR4 to stand healthier like those non-infected plants ((Fig. 5H-J). Notably, in addition to those DEGs well-known in phytoalexin accumulation and the plant's systemic immunity induction (Fig. 4D), genes encoding pathogenesis-related protein 1, chitinase, polyphenol oxidase, putative glucuronosyltransferase PGSIP8, 3-ketoacyl-CoA synthase, WRKY transcription factor and disease resistance protein RGA2, were found to be highly regulated (Fig. 5K) (Table S8). These genes have been reported to be highly expressed and critical in the immunity of wild bananas against *Fusarium* wilt (40). Collectively, exogenous supplementation of 100 nM PQQ in the early growing stage not only promotes the organ development of banana plantlets but also triggers the plant's systemic immunity, protecting bananas against *Fusarium* wilt either in tissue culture or in soil. These results suggested that the exogenous supplementation of PQQ to bananas in their early growth stage could contribute to triggering plant immune systems similar to wild bananas to combat *Fusarium* wilt, providing an untapped opportunity for in-field disease maintenance of the banana industry.

340 ## Discussion

341 **Molecular roles of endophytic PQQ in plant-microbe mutualisms**

342 On account of being a redox cofactor to types of dehydrogenases, PQQ participates
343 in multiple essential metabolisms across kingdoms. Several studies have reported its effects
344 on either prokaryotic or eukaryotic systems: acting as a strong antioxidant to scavenge
345 reactive oxygen species (41), regulating the balance of nicotinamide adenine dinucleotide
346 (9), inducing mitochondrial biogenesis (10, 11), driving the oxidative phosphorylation and
347 ATP synthesis (12, 13), etc. However, unlike microbes and animals, its molecular roles *in*
348 *planta* remains limited.

349 PQQ has been found to be produced by microbes, prevalent by Gram-negative
350 bacteria (42), and benefits the growth of some plants in different stages (16, 17, 43). In this
351 study, the PQQ exogenous supplementation on bananas and the follow-up transcriptomics
352 (Figs. 3,4) provided new materials and insights into its molecular effects in plants. Our
353 findings suggested that PQQ could affect mitochondrial and energetic metabolisms to
354 improve the overall growth of bananas (Figs. S7-S10), which echoed previous works on
355 animal cells. In addition, multiple phytohormone signalling pathways and photosynthesis of
356 banana plants were also found to be coordinated (Figs. 4,S17). These results provided
357 clues about the molecular roles of PQQ in plants and revealed the molecular roles of
358 endophytic PQQ in mutualistic relationships between plants and microbes.

359 On the other hand, research showed that the disruption of *pqq* genes causes the loss
360 of microbial antifungal activities (20, 21). Han et al. also determined the expression change
361 of a few genes participating in plant immunity, proposing the putative involvement of PQQ in
362 molecular plant-microbe-pathogen tripartite interactions (20). Herein, we confirmed that
363 PQQ has no anti-fungal activity *in vitro* (Fig. 2C) but induces plant immunity *in planta* to
364 protect banana plants against *Fusarium* wilt (Figs. 4-6,S17-S19). Interestingly, the seven
365 immune-related genes with continuously high expression levels of a commercial *Fusarium*-
366 resilient banana cultivar (40) were also found to be highly expressed within banana plants
367 after being treated with 100 nM PQQ (Fig. 5K) (Table S8). This result highlights the potential
368 of endophytic biostimulants, as PQQ here, in breeding biofortification or resistance that
369 achieves similar aims but via fewer costs, deserving more attention for future agriculture.

370

371 **Evolutionary and functional divergence of PQQ**

372 Although the chemical mechanisms of PQQ biosynthesis have been well studied
373 (44), the biosynthesis origin and evolution of this highly conserved order of open reading
374 frame within the *pqq* operon remain unclear. Shen et al. determined the distribution of the
375 main components*, i.e., pqqABCDE*, of the *pqq* operon over 126 prokaryotes (42). Similarly,
376 the *pqq* operon was identified from nearly all genomes of *Burkholderia* species, including

377 environmental isolates, pathogens and symbionts (Fig. 1). In this work, further comparative
378 genomics targeting the *pqq* operon was performed with the purpose of promoting our
379 understanding of such unclear evolutionary linkages between the species.

380 Interestingly, the result showed an environmental isolate *B. cenocepacia* BCMSMB
381 has two copies of the *pqq* operon (*pqqABCDE*, WL90_31170-31190 and *pqqBCDE*,
382 WL90_32390-32405) (Figs. 1B,S20). The incomplete operon was phylogenetically close to
383 *B. cenocepacia*, while the complete one was distinct to both species. Moreover, the
384 complete operon was further found to be located at a predicted gene island (Fig. S20B),
385 suggesting an occurrence of potential evolution events like inter-species horizontal gene
386 transfer. Besides, the *pqq* operon of a *B. seminalis* sub-group (BS0018+BS1628 clade)
387 seemed to get lost during their evolution. Further checking on the amino acid sequences of
388 the operon, a total of nine single amino acid polymorphisms (SAPs) between the species,
389 five in PqqB, two in PqqC and two in PqqE, were identified by multiple sequence alignment
390 (Fig. S21). The phylogenic trees constructed by amino acid sequences also distinguished
391 two species into different clades (Fig. S22). The catalyst within a PqqA/D/E complex is
392 considered the radical beginning of the PQQ biosynthesis, and the products of spontaneous
393 cyclisation after the PqqB-catalysed reaction is the substrate of PqqC in the final step of
394 PQQ biogenesis (44). Our comparative genomics revealed the potential evolutionary events
395 and phylogenic divergences of the operon, especially PqqB, PqqC and PqqE, of virulence
396 and non-virulence *Burkholderia* strains from different hosts and habitats. The results also
397 shed new light on studying the obscure roles of PQQ among molecular host-microbe
398 interactions and their evolution.

399 Moreover, distinct from participating as a cofactor for lactate dehydrogenase in
400 animal and microbial cells, our transcriptomic result suggested that PQQ mainly involve
401 regulations related to aldehydes and carboxylic acids in plant cells (Fig. 4D) (Table S7).
402 These differences may be due to the metabolic preference of lactate and ethanol
403 metabolisms in plant cells across the evolution and the results of host-symbiotic co-
404 evolution over time. A better understanding of such evolutionary and functional divergence
405 among lives is believed to provide great potential for academia and industry towards
406 sustainable agriculture. Beyond, some intriguing topics remain for future research, e.g., why
407 and how do non-PQQ-producing organisms, especially in eukaryotic cells like plants, utilise
408 PQQ? To better understand these questions, comprehensive investigations using integrated
409 approaches among PQQ participating host-microbe interactions are necessary for follow-up
410 research.

411

412 **Conclusion**

413 Previous studies showed the versatile benefits of endophytes to plants in promoting
414 host health and stress resistance (45–48). This work used multi-omics approaches and

415 imaging mass technologies to reveal a PQQ-involving arm racing among molecular plant-
416 endophyte-pathogen interactions. In summary, we demonstrated that *B. seminalis* 869T2
417 produces multiple biostimulants (*e.g.*, PQQ and cyclopeptides) and phytohormones (e.g.,
418 auxins, cytokinins, gibberellins, etc.) to improve the growth of host plants for symbiotic
419 relationships in general conditions; however, when host plants suffer from pathogens, it also
420 secrets antibiotics (*e.g.*, pyrrolnitrin and the derivates) to fight against the attackers (Fig. 2)
421 (Table S4,S5). Meanwhile, the PQQ induces plant immunity to promote the health and
422 resistance of the host plants, thus establishing an endophytic niche in defending those
423 pathogenic invaders (Fig. 6).

424 In conclusion, this is the first work through the omics landscape to explain how PQQ
425 involved plant-endophyte interactions and contributed to plant immunity. These results
426 facilitate our understanding of the realm and highlight PQQ as a potent biostimulant
427 candidate for future agriculture. Beyond the findings presented here, many intriguing
428 questions remain about PQQ in molecular plant-microbe interactions. Why and how do non-
429 PQQ-producing organisms utilize PQQ, particularly in plant cells and the organelles?
430 Further studies on their evolutionary and functional biology are expected to enhance our
431 understanding of this unique microbial redox cofactor in the future.

432

433 ## Materials and methods

434 ### Microbial and plant materials

435 The strain 869T2, *Fusarium oxysporum* f. sp. *cubense* tropical race 4 (*Foc* TR4) and
436 *Arabidopsis thaliana* ecotype Columbia (Col-0) seeds were retrieved from Chieh-Chen
437 Huang Lab's stocks. The plantlets of banana (*Musa acuminata* Cavendish cv. Pei-Chiao)
438 were purchased from Taiwan Banana Research Institute (TBRI), Pingtung, Taiwan.

439 ### Bacterial genome sequencing, assembly and annotation

440 The procedures for genome sequencing and analysis were based on those described
441 in our previous work on bacterial genomes (49–51). The same kits were used following the
442 manufacturer's protocols, and all bioinformatics tools were used with the default settings
443 unless stated otherwise.

444 Briefly, the total DNA of strain 869T2 was extracted and sequenced by Illumina
445 MiSeq 2 × 300 bp paired-end (MS-103-1003) and Oxford Nanopore Technologies (ONT)
446 MinION with R9.4 flow cell (FLO-MIN106) followed by Guppy v3.4.5 for basecalling. A
447 hybrid *de novo* assembly was produced using Unicycler v0.4.9-beta (52). For validation, the
448 Illumina and ONT raw reads were mapped to the assembly using BWA v0.7.12 (53) and
449 Minimap2 v2.15 (54). The results were programmatically checked using SAMtools v1.2 (55)
450 and manually inspected using IGV v2.3.57 (56). For assembly completeness evaluation, the
451 benchmarking universal single-copy orthologous (BUSCO) analysis with the Burkholderiales
452 dataset as a reference was executed on gVolante (57). The finalised assembly was
453 submitted to the National Center for Biotechnology Information (NCBI) and annotated using
454 their Prokaryotic Genome Annotation Pipeline (PGAP) (58). The KofamKOALA (59) was
455 further used to examine putative metabolic pathways.

456 ### Bacterial comparative genomics

457 The genome sequences of *Burkholderia* strains examined by Wallner *et al.* (36),
458 including closely related strains of *B. seminalis* and *B. cenocepacia*, plus an endophyte
459 strain *Paraburkholderia phytofirmans* PsJN (60), were retrieved from NCBI GenBank (61)
460 (accessed on 23 Jul 2021) for comparative analyses with 869T2 (Table S2). FastANI v1.124
461 (62) was used for whole-genome comparison to calculate the proportion of genomic
462 segments mapped and the average nucleotide identity (ANI). The homologous gene
463 clusters were identified using OrthoMCL v1.3 (63) for maximum likelihood phylogeny
464 construction and gene content analysis. These genes were used to produce a concatenated
465 alignment using MUSCLE v3.8.31 (64) for maximum-likelihood inference by PhyML
466 v.3.3.20180214 (65) and visualised using FigTree v1.4.4. PHYLIP v3.69723 (66) was used
467 for bootstrap analysis. For gene content analysis, the previously reported human virulence-
468 facilitating (VIR) and environmental adaptation and MPMI (ENV) related genes were mainly
469 targeted (36). *B. cenocepacia* J2315^{T} and *B. seminalis* LMG24067^{T} were set as the default

470 reference for the VIR and ENV checks, respectively. Given several incomplete genomes
471 were included and the genetic complexity of the *Burkholderia cepacia* complex (BCC),
472 besides homologous gene clusters inferred by OrthoMCL, an additional manual check on
473 the gene length and annotation was also carried out with BLASTP v2.6.0 (67) with e-value
474 cut-off set to 1e-15 and the amino acid sequence identity cut-off set to 80%. Lists of
475 targeted genes for gene content analysis were provided as supporting information (Table
476 S3).

477 **Imaging mass spectrometry analysis**

478 Strain 869T2 was first incubated in LB media at 28°C for 24 hours and then
479 transplanted 2 μL of bacterial culture to a PDA plate as a spot. The spot was incubated
480 alone, or a 4 mm mycelial plug of *Foc* TR4 from a 7-day fungal plate was placed at the
481 opposite edge of the bacterial spot for the dual incubation for five days to monitor the
482 metabolic changes by using matrix-assisted laser desorption/ionisation (MALDI) time-of-
483 flight (TOF) imaging mass spectrometry (IMS). All procedures and settings followed the
484 previously described unless otherwise stated (68, 69). Briefly, the sample areas of agar
485 containing the bacteria alone or with fungal mycelia were excised and transferred onto the
486 MALDI stainless steel target plate. A 1:1 mixture of α-cyano-4-hydroxycinnamic acid and
487 2,5-dihydroxybenzoic acid (universal matrix, Sigma-Aldrich) was spread on top of the
488 samples, then exposed in a 37˚C incubator overnight until it was deemed dried. The IMS
489 data were collected using a Bruker Autoflex Speed MALDI-TOF/TOF mass spectrometer
490 (Bruker Daltonik GmbH, Bremen, Germany) with the following setting: 1000 shots/raster,
491 19.0 and 16.6 kV for the ion sources 1 and 2, 8.7 kV for the lens, 21 and 9.4 kV for
492 reflectors 1 and 2, respectively. The mass ranges from m/z 100-2000 with 25% laser power,
493 positive and reflectron mode was selected, and the raster was set to 800 μm. The universal
494 matrix and peptide standard I (Bruker Daltonik GmbH, Bremen, Germany) were used for MS
495 calibration. All IMS data were processed with TIC normalisation mode and analysed using
496 Fleximaging 3.3 (Bruker Daltonik GmbH, Bremen, Germany).

497 ***In vitro* antagonism assay**

498 The *in vitro* anti-*Fusarium* activity was assessed by comparing fungal hyphal growth
499 rates under the presence and absence of the examined targets. All procedures followed
500 previous work (28) with minor modifications. Strain 869T2 was set as the positive control,
501 and the ddH_2O was used as the mocking negative control. Three concentrations of PQQ
502 (10^2, 10^4 and 10^6 nM) were examined. The antagonistic plate images were photographed,
503 the fungal hyphal growth was measured through ImageJ (70), and the antifungal efficiency
504 (AE) was calculated by AE = (DC-DT)/DC x 100%. DC and DT are *Foc* TR4 colony
505 diameters of the negative control and the comparing target, respectively.

506 **Exogenous supplementation of pyrroloquinoline quinone to plants**

507 The banana plantlets were grown with MS media in the NCHU plant growth chamber
508 as previously described (28) with synthetic PQQ supplementation in different concentrations
509 (Experiment I: 0, 5, 50, 100 and 1000 nM; Experiment II: 0, 100, 1000 and 2000 nM).
510 Phenotypes were photographed, and the growth indicators of visible root formation rate,
511 average leaves number and distribution, plant height, fresh weight, etc., were recorded to
512 determine the plant-growth-promoting (PGP) effects and efficient working dosage of PQQ in
513 plants. Besides, the PQQ-treated banana plantlets were normalised and then transplanted
514 into soil pots, moved to the NCHU greenhouse as described above, and then used for the
515 following *Fusarium* infection assay.

516 ***Fusarium* infection assay and Panama disease resistance evaluation**

517 All procedures of the infection assay carried out in tissue culture containers or soil
518 pots were followed in previous works (28) unless otherwise stated. *Foc* TR4 infectious
519 inocula were prepared in a final concentration of 10^6 conidia per mL. For the tissue culture
520 system, a 5 mm diameter filter paper disc soaked within the infectious inocula was placed at
521 the centre of the banana plantlets for the infection. For the soil pot system, the bananas
522 were domesticated in the NCHU greenhouse and then infected by transplantation into pots
523 containing *Foc* TR4, with a final concentration of 2.8×10^3 spores per gram of soil. The
524 planting matrixes prepared with and without *Foc* TR4 were set as the positive (CKp = CKp2)
525 and negative control (CKn = CKn2), respectively. Four indicators of Panama disease, *i.e.*,
526 leaf yellowing (LY), pseudostem splitting (SS), rhizome (RB) and pseudostem dark brown
527 discolouration (SB) (71), and plant morbidity were determined three months after the
528 infection. Plants without and with LY/SS/SB were recorded as 0 and 1, respectively; plants
529 with RB were recorded as 0, 1, 2 and 3 according to the severity of none, low, medium and
530 high (72); dead plants were weighted by adding 1 to the total score. The fully-scored virtual
531 positive control (CKp1) and zero-scored virtual negative control (CKn1) were also included
532 to assist the follow-up analyses.

533 The principal component analysis (PCA) and the unweighted pair group method with
534 arithmetic mean (UPGMA) were used to analyse the above score data to evaluate the
535 contribution of exogenous supplementation of PQQ to Panama disease resistance. The
536 statistical analyses were performed in R version 4.3.2 (73). For PCA, the function prcomp()
537 was used for primary analysis, and the result was plotted by using the function
538 fviz_pca_biplot(). For UPGMA, the function pvclust() with the distancing method of
539 "Euclidean", hierarchical clustering method of "average", and 1,000 times multiscale
540 bootstrap re-samplings were performed. FigTree v1.4.4 was used for the tree visualisation.
541 To test the effect of the clustering method, we also used the function dist() for calculating
542 the Euclidean distancing-based similarity matrix calculation, then used the function upgma()
543 to construct the dendrogram. As both alternatives produced the same clustering suggestion,
544 only the result based on the pvclust() method with multiscale bootstrap analysis was
545 reported.

546 **Plant total RNA extraction and transcriptomic analysis**

547 The RNA sequencing and analysis procedures were based on those presented in our
548 previous works on plant transcriptomics (50, 72, 74). All kits were used according to the
549 manufacturer's protocols, and all bioinformatics tools were used with the default settings
550 and followed Welgene Biotech's in-house pipeline unless stated otherwise. Banana plantlets
551 were harvested after 11 weeks and grown in ½ MS media with the 100 nM PQQ (treatment)
552 and without PQQ (control), respectively. Total RNA was extracted from the mixtures of three
553 bananas for each treatment using Trizol reagent. The library constructions were generated
554 using TruSeq Stranded mRNA Library Prep Kit (RS-122-2101; Illumina, San Diego, CA
555 USA) and assessed to Agilent Bioanalyzer 2100 system using DNA High Sensitivity Chips
556 for qualification. Illumina Hiseq 4000 platform was used for 150-bp paired-end sequencing.
557 Illumina's program bcl2fastq v2.20 was used for basecalling, and Trimmomatic v0.3642 (75)
558 was implemented to trim off low-quality reads based on Q20 accuracy. The resultant was
559 mapped to *Musa acuminata* subsp. *malaccensis* (NCBI: txid214687) genome (76) using
560 HISAT2 (77). The transcript per million (TPM) method was used for normalisation; genes
561 with low expression levels (< 0.3 TPM value) were excluded. Genes with at least 2.0-fold
562 differences and a probability of at least 0.95 were defined as differentially expressed genes
563 (DEGs). StringTie v2.1.4 (78) and DEseq2 v1.28.1 (79) were used for genome bias
564 detection/correction. Gene set enrichment analysis (GSEA) (80), Gene Ontology (GO) (81)
565 and Kyoto Encyclopedia of Genes and Genomes (KEGG) databases (82) were accessed
566 for the metabolic analyses.

567 **Statistics**

568 The Shapiro-Wilk test and Levene's test were used to check the normal distribution
569 of variables and homoscedasticity, respectively. One-way ANOVA analysis with Tukey's
570 post hoc HSD test for parametric analysis or Kruskal-Wallis test with Dunn's post hoc test
571 for non-parametric analysis was performed to estimate the statistical significance between
572 samples. The data analysis was performed using the Real Statistics Resource Pack v7.7.1
573 (83). At least three independent biological replicates were tested for all experiments, and
574 data are mainly shown as mean ± SE. *$P \leq 0.05$, **$P \leq 0.01$, ***$P \leq 0.005$ and ****$P \leq 0.001$
575 indicated significant differences between samples; otherwise, no significance.

576

Acknowledgements

The Illumina MiSeq and ONT MinION sequencing services for bacterial genome was provided by the Genomic Technology Core (Institute of Plant and Microbial Biology, Academia Sinica). The RNA-seq services were provided by Welgene Biotech Co., Ltd. (Taipei, Taiwan) and Genomics BioSci & Tech Co., Ltd. (Taipei, Taiwan). We thank the technical assistance and the support from Taiwan Banana Research Institute (TBRI), Pingtung, Taiwan and Taichung District Agricultural Research and Extension Station, Ministry of Agriculture of Taiwan.

Author Contributions

SHWH, MYY and CCH designed research; CCH and CHK acquired funding; CCH supervised the project; SHWH, MYY, CHL, TCH, JHP and YNH performed research; SHWH, CHL, TCH, JHP and YNH analysed data; SHWH wrote the paper - original draft; SHWH, JHP, NYJ, CHK, YNH, EPIC, HHH and CCH wrote the paper - review & editing.

Funding

This work was supported by the National Science and Technology Council of Taiwan (MOST 107-2321-B-005-009; MOST 108-2321-B-005-004; MOST 109-2321-B-005-025; MOST 110-2321-B-005-008), the Ministry of Agriculture of Taiwan (110AS-1.6.1-BQ-B3), and the Ministry of Education of Taiwan (the Higher Education Sprout Project) to Chieh-Chen Huang and Academia Sinica to Chih-Horng Kuo. The funders had no role in study design, data collection and interpretation, or the decision to submit the work for publication.

Data availability

The complete genome sequence of *Burkholderia seminalis* 869T2 has been deposited in GenBank under the accession numbers CP072520-22. The bacterial genome and the plant transcriptome sequencing project, including the associated raw reads, have been deposited in the NCBI under BioProject PRJNA243842 and BioProject PRJNA786465, respectively.

603 ## References

604 1. J. G. Hauge, Kinetics and specificity of glucose dehydrogenase from Bacterium
605 anitratum. *Biochimica et Biophysica Acta* **45**, 263–269 (1960).

606 2. S. A. Salisbury, H. S. Forrest, W. B. T. Cruse, O. Kennard, A novel coenzyme from
607 bacterial primary alcohol dehydrogenases. *Nature* **280**, 843–844 (1979).

608 3. L. Chistoserdova, S.-W. Chen, A. Lapidus, M. E. Lidstrom, Methylotrophy in
609 Methylobacterium extorquens AM1 from a genomic point of view. *J Bacteriol* **185**,
610 2980–2987 (2003).

611 4. J. A. Duine, The PQQ story. *J Biosci Bioeng* **88**, 231–236 (1999).

612 5. M. Matsutani, T. Yakushi, Pyrroloquinoline quinone-dependent dehydrogenases of
613 acetic acid bacteria. *Appl Microbiol Biotechnol* **102**, 9531–9540 (2018).

614 6. M. Naveed, K. Tariq, H. Sadia, H. Ahmad, A. S. Mumtaz, The life history of
615 pyrroloquinoline quinone (pqq): a versatile molecule with novel impacts on living
616 systems. *IJMBOA* **1**, 29–46 (2016).

617 7. C. Anthony, Pyrroloquinoline quinone (PQQ) and quinoprotein enzymes. *Antioxid*
618 *Redox Signal* **3**, 757–774 (2001).

619 8. P. M. Goodwin, C. Anthony, The biochemistry, physiology and genetics of PQQ and
620 PQQ-containing enzymes. *Adv Microb Physiol* **40**, 1–80 (1998).

621 9. K. R. Jonscher, W. Chowanadisai, R. B. Rucker, Pyrroloquinoline-quinone is more than
622 an antioxidant: a vitamin-like accessory factor important in health and disease
623 prevention. *Biomolecules* **11**, 1441 (2021).

624 10. W. Chowanadisai, *et al.*, Pyrroloquinoline Quinone Stimulates Mitochondrial Biogenesis
625 through cAMP Response Element-binding Protein Phosphorylation and Increased
626 PGC-1α Expression*. *Journal of Biological Chemistry* **285**, 142–152 (2010).

627 11. K. Saihara, R. Kamikubo, K. Ikemoto, K. Uchida, M. Akagawa, Pyrroloquinoline
628 Quinone, a Redox-Active o-Quinone, Stimulates Mitochondrial Biogenesis by Activating
629 the SIRT1/PGC-1α Signaling Pathway. *Biochemistry* **56**, 6615–6625 (2017).

630 12. A. Canovai, *et al.*, Pyrroloquinoline quinone drives ATP synthesis in vitro and in vivo
631 and provides retinal ganglion cell neuroprotection. *Acta Neuropathologica*
632 *Communications* **11**, 146 (2023).

633 13. M. C. Ebeling, *et al.*, Improving retinal mitochondrial function as a treatment for age-
634 related macular degeneration. *Redox Biology* **34**, 101552 (2020).

14. R. Carreño-López, J. M. Alatorre-Cruz, V. Marín-Cevada, “Pyrroloquinoline quinone (PQQ): role in plant-microbe interactions” in *Secondary Metabolites of Plant Growth Promoting Rhizomicroorganisms: Discovery and Applications*, H. B. Singh, C. Keswani, M. S. Reddy, E. Sansinenea, C. García-Estrada, Eds. (Springer, 2019), pp. 169–184.

15. M. Ben Farhat, A. Fourati, H. Chouayekh, Coexpression of the pyrroloquinoline quinone and glucose dehydrogenase genes from Serratia marcescens CTM 50650 conferred high mineral phosphate-solubilizing ability to Escherichia coli. *Appl Biochem Biotechnol* **170**, 1738–1750 (2013).

16. Y.-S. Cho, *et al.*, PQQ-dependent organic acid production and effect on common bean growth by Rhizobium tropici CIAT 899. *Journal of Microbiology and Biotechnology* **13**, 955–959 (2003).

17. O. Choi, *et al.*, Pyrroloquinoline quinone is a plant growth promotion factor produced by Pseudomonas fluorescens B16. *Plant Physiol* **146**, 657–668 (2008).

18. L. Li, Z. Jiao, L. Hale, W. Wu, Y. Guo, Disruption of gene pqqA or pqqB reduces plant growth promotion activity and biocontrol of crown gall disease by Rahnella aquatilis HX2. *PLoS One* **9**, e115010 (2014).

19. A. H. Patel, V. Chovatia, S. Shah, Expression of pyrroloquinoline quinone in Rhizobium leguminosarum for phosphate solubilization. *Environment and Ecology* **33**, 621–624 (2015).

20. S. H. Han, *et al.*, Inactivation of pqq genes of Enterobacter intermedium 60-2G reduces antifungal activity and induction of systemic resistance. *FEMS Microbiol Lett* **282**, 140–146 (2008).

21. J. Xu, *et al.*, The pqqC gene is essential for antifungal activity of Pseudomonas kilonensis JX22 against Fusarium oxysporum f. sp. lycopersici. *FEMS Microbiology Letters* **353**, 98–105 (2014).

22. F. Garcia-Bastidas, Fusarium oxysporum f.sp. cubense tropical race 4 (Foc TR4). *CABI Compendium* **CABI Compendium**, 59074053 (2022).

23. R. C. Ploetz, Fusarium Wilt of Banana. *Phytopathology®* **105**, 1512–1521 (2015).

24. TR4 Global Network, TR4 Basics. Available at https://www.fao.org/tr4gn/tr4-basics/en/. Deposited 15 January 2024.

25. A. A. Ismaila, *et al.*, Fusarium wilt of banana: Current update and sustainable disease control using classical and essential oils approaches. *Horticultural Plant Journal* **9**, 1–28 (2023).

26. G. Bubici, M. Kaushal, M. I. Prigigallo, C. Gómez-Lama Cabanás, J. Mercado-Blanco, Biological Control Agents Against Fusarium Wilt of Banana. *Frontiers in Microbiology* **10**, 616 (2019).

27. C. Du, *et al.*, Construction of a compound microbial agent for biocontrol against Fusarium wilt of banana. *Frontiers in Microbiology* **13**, 1066807 (2022).

28. Y.-N. Ho, *et al.*, In planta biocontrol of soilborne Fusarium wilt of banana through a plant endophytic bacterium, Burkholderia cenocepacia 869T2. *Plant Soil* **387**, 295–306 (2015).

29. Z. Zhu, *et al.*, Spatiotemporal biocontrol and rhizosphere microbiome analysis of Fusarium wilt of banana. *Commun Biol* **6**, 1–10 (2023).

30. T. Damodaran, *et al.*, Secondary metabolite induced tolerance to Fusarium oxysporum f.sp. cubense TR4 in banana cv. Grand Naine through in vitro bio-immunization: a prospective research translation from induction to field tolerance. *Frontiers in Microbiology* **14**, 1233469 (2023).

31. L. Zhang, *et al.*, Biocontrol Potential of Endophytic Streptomyces malaysiensis 8ZJF-21 From Medicinal Plant Against Banana Fusarium Wilt Caused by Fusarium oxysporum f. sp. cubense Tropical Race 4. *Frontiers in Plant Science* **13**, 874819 (2022).

32. Y.-N. Ho, C.-C. Huang, Draft genome sequence of Burkholderia cenocepacia strain 869T2, a plant-beneficial endophytic bacterium. *Genome Announcements* **3**, e01327-15 (2015).

33. H.-H. Hwang, *et al.*, A plant endophytic bacterium, Burkholderia seminalis strain 869T2, promotes plant growth in Arabidopsis, Pak Choi, Chinese amaranth, lettuces, and other vegetables. *Microorganisms* **9**, 1703 (2021).

34. S.-H. W. Hung, *et al.*, Endophytic biostimulants for smart agriculture: Burkholderia seminalis 869T2 benefits heading leafy vegetables in-field management in Taiwan. *Agronomy* **13**, 967 (2023).

35. B.-A. T. Nguyen, *et al.*, Biodegradation of dioxins by Burkholderia cenocepacia strain 869T2: role of 2-haloacid dehalogenase. *Journal of Hazardous Materials* **401**, 123347 (2021).

36. A. Wallner, E. King, E. L. M. Ngonkeu, L. Moulin, G. Béna, Genomic analyses of Burkholderia cenocepacia reveal multiple species with differential host-adaptation to plants and humans. *BMC Genomics* **20**, 803 (2019).

37. A. Baldwin, P. A. Sokol, J. Parkhill, E. Mahenthiralingam, The Burkholderia cepacia epidemic strain marker is part of a novel genomic island encoding both virulence and

702 metabolism-associated genes in Burkholderia cenocepacia. *Infect Immun* **72**, 1537–
703 1547 (2004).

704 38. S. Pawar, A. Chaudhari, R. Prabha, R. Shukla, D. P. Singh, Microbial Pyrrolnitrin:
705 Natural Metabolite with Immense Practical Utility. *Biomolecules* **9**, 443 (2019).

706 39. Y. B. Guo, *et al.*, Mutations That Disrupt Either the pqq or the gdh Gene of Rahnella
707 aquatilis Abolish the Production of an Antibacterial Substance and Result in Reduced
708 Biological Control of Grapevine Crown Gall. *Applied and Environmental Microbiology*
709 **75**, 6792–6803 (2009).

710 40. L. Zhang, *et al.*, Transcriptomic analysis of resistant and susceptible banana corms in
711 response to infection by Fusarium oxysporum f. sp. cubense tropical race 4. *Sci Rep* **9**,
712 8199 (2019).

713 41. H. S. Misra, *et al.*, Pyrroloquinoline-quinone: a reactive oxygen species scavenger in
714 bacteria. *FEBS Letters* **578**, 26–30 (2004).

715 42. Y.-Q. Shen, *et al.*, Distribution and properties of the genes encoding the biosynthesis of
716 the bacterial cofactor, pyrroloquinoline quinone. *Biochemistry* **51**, 2265–2275 (2012).

717 43. L. B. Xiong, J. Sekiya, N. Shimose, Occurrence of Pyrroloquinoline Quinone (PQQ) in
718 Pistils and Pollen Grains of Higher Plants. *Agricultural and Biological Chemistry* **54**,
719 249–250 (1990).

720 44. Zhu, J. P. Klinman, Biogenesis of the peptide-derived redox cofactor pyrroloquinoline
721 quinone. *Current Opinion in Chemical Biology* **59**, 93–103 (2020).

722 45. S. Card, L. Johnson, S. Teasdale, J. Caradus, Deciphering endophyte behaviour: the
723 link between endophyte biology and efficacious biological control agents. *FEMS*
724 *Microbiol Ecol* **92**, fiw114 (2016).

725 46. P. Chaudhary, U. Agri, A. Chaudhary, A. Kumar, G. Kumar, Endophytes and their
726 potential in biotic stress management and crop production. *Frontiers in Microbiology*
727 **13**, 933017 (2022).

728 47. J. Hallmann, A. Quadt-Hallmann, W. F. Mahaffee, J. W. Kloepper, Bacterial
729 endophytes in agricultural crops. *Can. J. Microbiol.* **43**, 895–914 (1997).

730 48. P. R. Hardoim, *et al.*, The hidden world within plants: ecological and evolutionary
731 considerations for defining functioning of microbial endophytes. *Microbiol Mol Biol Rev*
732 **79**, 293–320 (2015).

733 49. S.-H. W. Hung, M.-C. Chiu, C.-C. Huang, C.-H. Kuo, Complete genome sequence of
734 Curtobacterium sp. C1, a beneficial endophyte with the potential for in-plant salinity
735 stress alleviation. *MPMI* **35**, 731–735 (2022).

736 50. S.-H. W. Hung, *et al.*, A cyclic dipeptide for salinity stress alleviation and the trophic
737 flexibility of endophyte provide insights into saltmarsh plant–microbe interactions. *ISME*
738 *Communications* **4**, ycae041 (2024).

739 51. S.-H. W. Hung, I.-C. Wu, C.-C. Huang, C.-H. Kuo, Complete genome sequence of
740 Erythrobacteraceae bacterium WH01K, a strain isolated from corals (Acropora sp.) in
741 Taiwan. *Microbiology Resource Announcements* **12**, e00830-23 (2023).

742 52. R. R. Wick, L. M. Judd, C. L. Gorrie, K. E. Holt, Unicycler: resolving bacterial genome
743 assemblies from short and long sequencing reads. *PLoS Comput Biol* **13**, e1005595
744 (2017).

745 53. H. Li, R. Durbin, Fast and accurate short read alignment with Burrows-Wheeler
746 transform. *Bioinformatics* **25**, 1754–1760 (2009).

747 54. H. Li, Minimap2: pairwise alignment for nucleotide sequences. *Bioinformatics* **34**,
748 3094–3100 (2018).

749 55. H. Li, *et al.*, The sequence alignment/map format and SAMtools. *Bioinformatics* **25**,
750 2078–2079 (2009).

751 56. J. T. Robinson, *et al.*, Integrative genomics viewer. *Nat Biotechnol* **29**, 24–26 (2011).

752 57. O. Nishimura, Y. Hara, S. Kuraku, Evaluating genome assemblies and gene models
753 using gVolante. *Methods Mol Biol* **1962**, 247–256 (2019).

754 58. T. Tatusova, *et al.*, NCBI prokaryotic genome annotation pipeline. *Nucleic Acids Res*
755 **44**, 6614–6624 (2016).

756 59. T. Aramaki, *et al.*, KofamKOALA: KEGG Ortholog assignment based on profile HMM
757 and adaptive score threshold. *Bioinformatics* **36**, 2251–2252 (2020).

758 60. A. Weilharter, *et al.*, Complete genome sequence of the plant growth-promoting
759 endophyte Burkholderia phytofirmans strain PsJN. *Journal of Bacteriology* **193**, 3383–
760 3384 (2011).

761 61. D. A. Benson, *et al.*, GenBank. *Nucleic Acids Res* **46**, D41–D47 (2018).

762 62. C. Jain, L. M. Rodriguez-R, A. M. Phillippy, K. T. Konstantinidis, S. Aluru, High
763 throughput ANI analysis of 90K prokaryotic genomes reveals clear species boundaries.
764 *Nat Commun* **9**, 5114 (2018).

765 63. L. Li, C. J. Stoeckert, D. S. Roos, OrthoMCL: identification of ortholog groups for
766 eukaryotic genomes. *Genome Res.* **13**, 2178–2189 (2003).

767 64. R. C. Edgar, MUSCLE: multiple sequence alignment with high accuracy and high
768 throughput. *Nucleic Acids Research* **32**, 1792–1797 (2004).

769 65. S. Guindon, O. Gascuel, A simple, fast, and accurate algorithm to estimate large
770 phylogenies by maximum likelihood. *Systematic Biology* **52**, 696–704 (2003).

771 66. J. Felsenstein, PHYLIP - phylogeny inference package (version 3.2). *Cladistics* **5**, 164–
772 166 (1989).

773 67. C. Camacho, *et al.*, BLAST+: architecture and applications. *BMC Bioinformatics* **10**,
774 421 (2009).

775 68. Y.-N. Ho, *et al.*, Specific inactivation of an antifungal bacterial siderophore by a fungal
776 plant pathogen. *ISME J* **15**, 1858–1861 (2021).

777 69. Y.-L. Yang, Y. Xu, P. Straight, P. C. Dorrestein, Translating metabolic exchange with
778 imaging mass spectrometry. *Nat Chem Biol* **5**, 885–887 (2009).

779 70. C. A. Schneider, W. S. Rasband, K. W. Eliceiri, NIH image to ImageJ: 25 years of
780 image analysis. *Nat Methods* **9**, 671–675 (2012).

781 71. Y. Wu, *et al.*, Systemic acquired resistance in Cavendish banana induced by infection
782 with an incompatible strain of Fusarium oxysporum f. sp. cubense. *Journal of Plant*
783 *Physiology* **170**, 1039–1046 (2013).

784 72. M.-Y. Yu, “A study of pyrroloquinoline quinone on Pei-Chiao (Musa spp.) growth and
785 biocontrol improvement,” National Chung Hsing University, Taichung, Taiwan. (2019).

786 73. R Core Team, R: A Language and Environment for Statistical Computing. (2024).
787 Deposited 18 March 2024.

788 74. Y.-H. Tsai, “Transcriptomic analysis on adaptive immunity of Pei-Chiao (Musa spp.,
789 Cavendish AAA) against Fusarium wilt caused by Fusarium oxysporum f. sp. cubense
790 tropical race4.,” National Chung Hsing University, Taichung, Taiwan. (2019).

791 75. A. M. Bolger, M. Lohse, B. Usadel, Trimmomatic: a flexible trimmer for Illumina
792 sequence data. *Bioinformatics* **30**, 2114–2120 (2014).

793 76. A. D’Hont, *et al.*, The banana (Musa acuminata) genome and the evolution of
794 monocotyledonous plants. *Nature* **488**, 213–217 (2012).

795 77. D. Kim, B. Langmead, S. L. Salzberg, HISAT: a fast spliced aligner with low memory
796 requirements. *Nat Methods* **12**, 357–360 (2015).

797 78. M. Pertea, *et al.*, StringTie enables improved reconstruction of a transcriptome from
798 RNA-seq reads. *Nat Biotechnol* **33**, 290–295 (2015).

799 79. M. I. Love, W. Huber, S. Anders, Moderated estimation of fold change and dispersion
800 for RNA-seq data with DESeq2. *Genome Biology* **15**, 550 (2014).

801 80. A. Subramanian, *et al.*, Gene set enrichment analysis: A knowledge-based approach
802 for interpreting genome-wide expression profiles. *Proc. Natl. Acad. Sci. U.S.A.* **102**,
803 15545–15550 (2005).

804 81. H. Mi, A. Muruganujan, D. Ebert, X. Huang, P. D. Thomas, PANTHER version 14: more
805 genomes, a new PANTHER GO-slim and improvements in enrichment analysis tools.
806 *Nucleic Acids Research* **47**, D419–D426 (2019).

807 82. M. Kanehisa, S. Goto, KEGG: Kyoto encyclopedia of genes and genomes. *Nucleic*
808 *Acids Res* **28**, 27–30 (2000).

809 83. C. Zaiontz, Real Statistics Resource Pack software. Available at www.real-
810 statistics.com. Deposited 21 February 2024.

811

Figure Legends

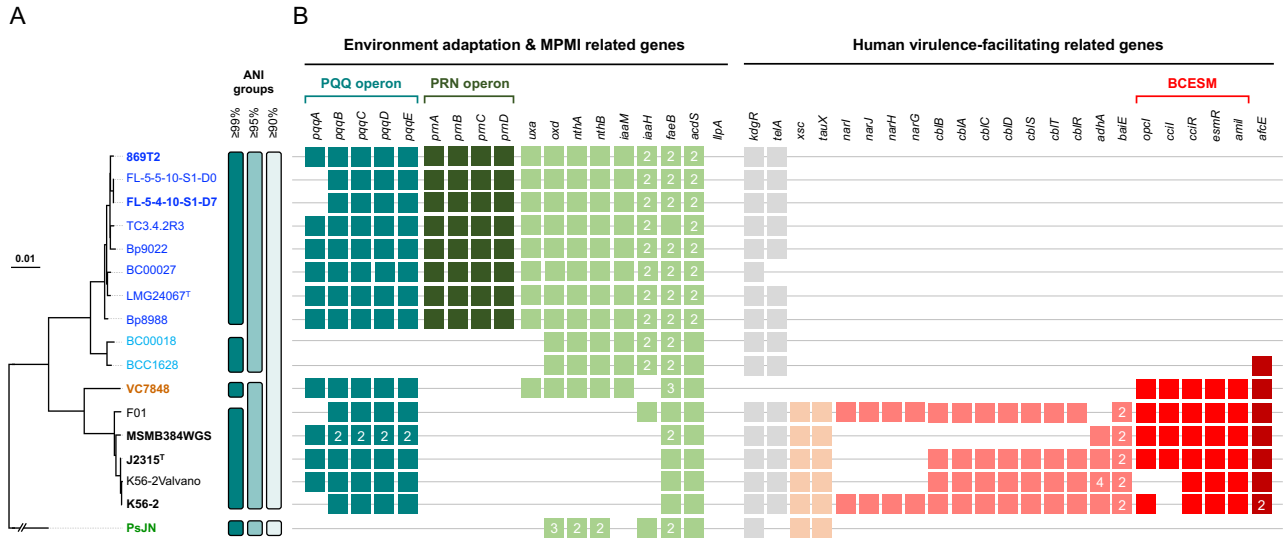

Fig. 1 Evolutionary and comparative genomics among strain 869T2 and its relatives. A Maximum likelihood phylogeny based on a concatenated alignment of 3,018 single-copy genes shared by all genomes (987,390 aligned amino acid sites). All internal nodes received 100% bootstrap support based on 1,000 resamplings. *Paraburkholderia phytofirmans* PsJN^{T} is included as the outgroup. The superscripts 'T' following the strain names indicate type strains and the complete genomes are presented in bold. Grouping based on different genome-wide average nucleotide identity (ANI) thresholds is plotted to the right of the phylogenic tree. **B** Gene content analysis. The distribution of key genes involved in environmental adaptation, molecular plant-microbe interactions (MPMI), and human virulence-facilitating (VIR) are plotted. The colour boxes indicate gene presence, and the numbers within the boxes indicate copy numbers of multi-copy genes. Abbreviations: PQQ, pyrroloquinoline quinone. PRN, pyrrolnitrin. BCESM, *Burkholderia cepacia* epidemic strain marker. Detailed information regarding the strains and target genes are provided in Table S2 and Table S3, respectively.

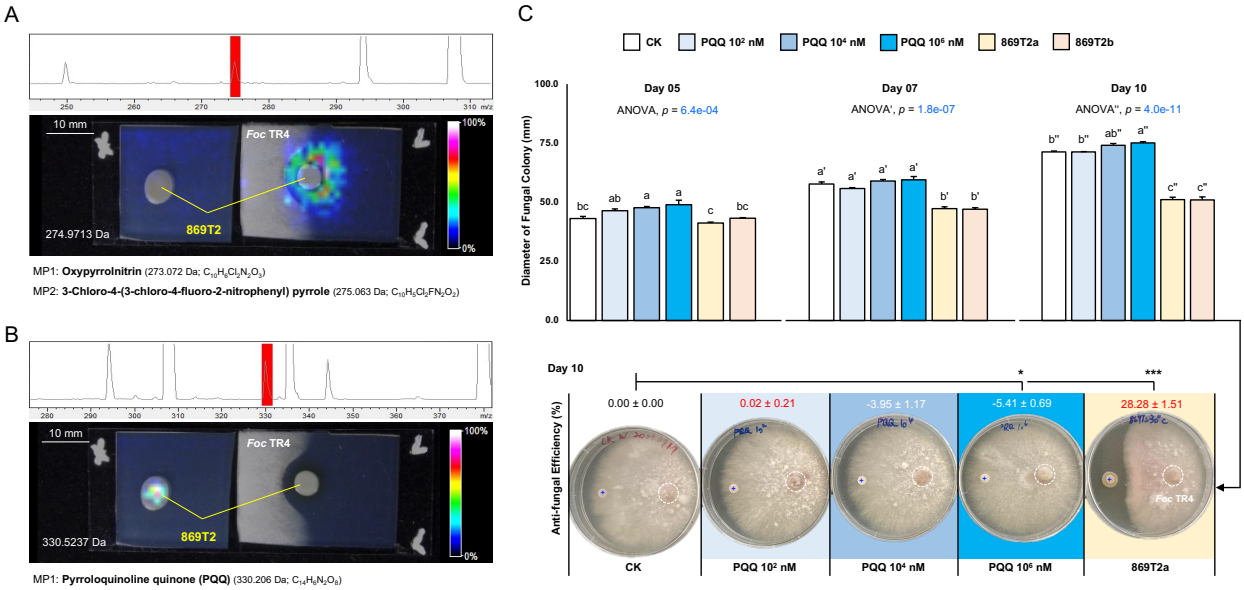

Fig. 2 Identification and quantification of potential endophytic biostimulants. *In situ* imaging mass results of endophyte-pathogen co-incubation under the metabolic signalling detection under **A** 274.9713 m/z and **B** 330.5237 m/z, respectively. 869T2, *Burkholderia seminalis* 869T2. *Foc* TR4, *Fusarium oxysporum* f. sp. cubense tropical race 4. MP, metabolite of prediction. Colour keys refer to the metabolic abundance of detection. **C** Antagonism assay for testing different concentrations of pyrroloquinoline quinone (PQQ) against *Foc* TR4 *in vitro*. PQQ was prepared as 10^2, 10^4, and 10^6 nM for the assay. *Burkholderia seminalis* 869T2 precultured under precultured under 30°C (869T2a) or 37°C (869T2b) was set as the positive control, and the ddH_2O was set as the negative control (CK). The sample disk of each treatment and Foc TR4 were highlighted by a blue cross and a white dashed circle, respectively, within the plate images. Data were presented as mean ± SEM, N = 3. Statistical significances between samples were indicated by different letters ($p<0.05$) or by asterisks (*$p<0.05$; ***$p<0.005$); otherwise, not significant.

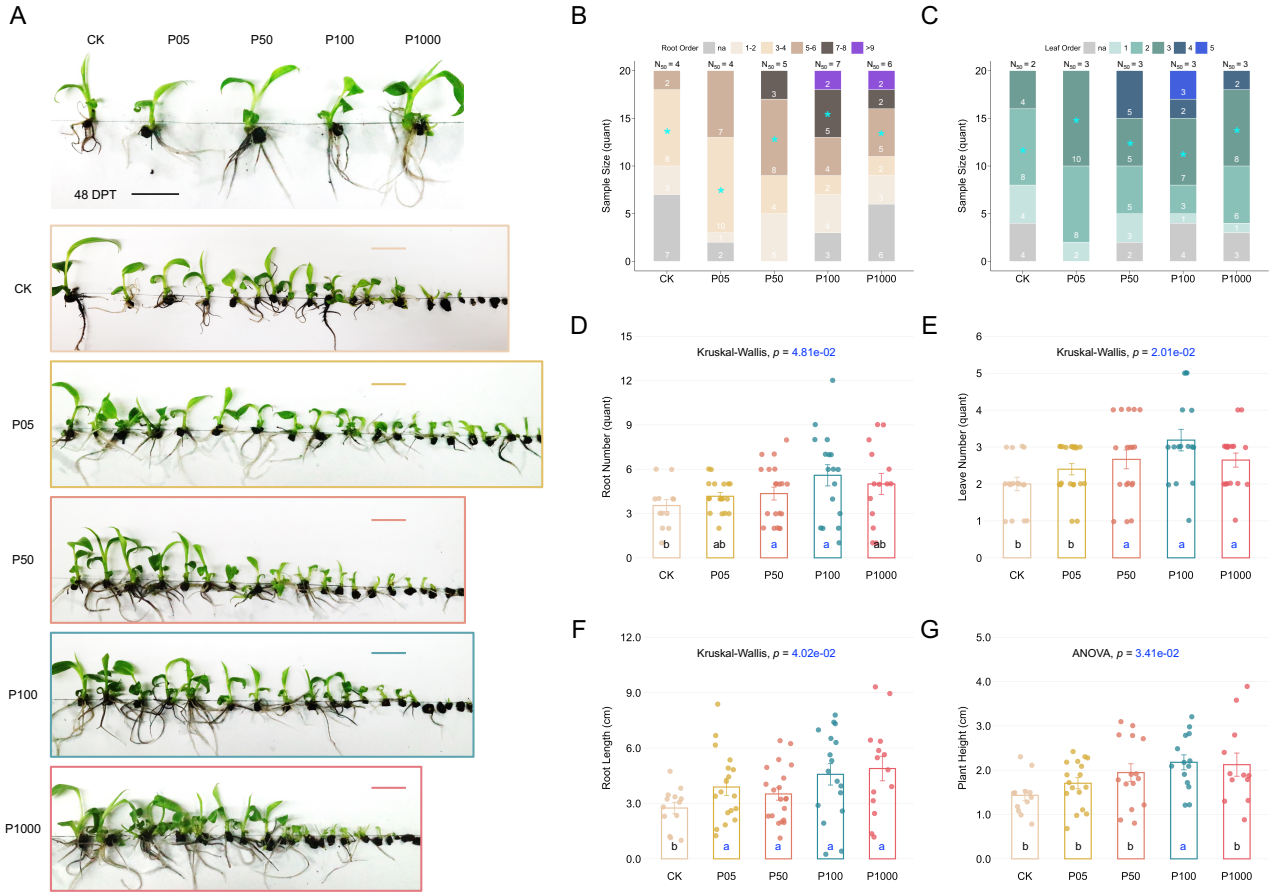

Fig. 3 Exogenous supplementation of PQQ benefits the differentiation and development of banana plants in tissue culture conditions. A Phenotypic photographs of banana plants in response to different concentrations of supplementary pyrroloquinoline quinone (PQQ) at 48 days after treatment (DPT). CK, P05, P50, P100 and P1000 indicate the 0 nM, 5 nM, 50 nM, 100 nM and 1000 nM PQQ treatment, respectively. Scale bars, 3 cm. The distribution of **B** root number and **C** leaf number of banana plants at 48 DPT. Numbers in stacked bar charts indicate the sample size. Asterisks highlight the distribution groups of defined N_{50} for plant growth-promotion evaluation, as mentioned in Materials and Methods. na, non-differentiated samples. **D** Root number, **E** leaf number, **F** root length and **G** plant height of banana plants at 48 DPT, excluding non-differentiated samples in **B** or **C**. Each dot represents a sample. Data are mean ± SEM; different letters indicate significant differences based on multiple comparisons, Tukey method after ANOVA or Dunn method after the Kruskal-Wallis test.

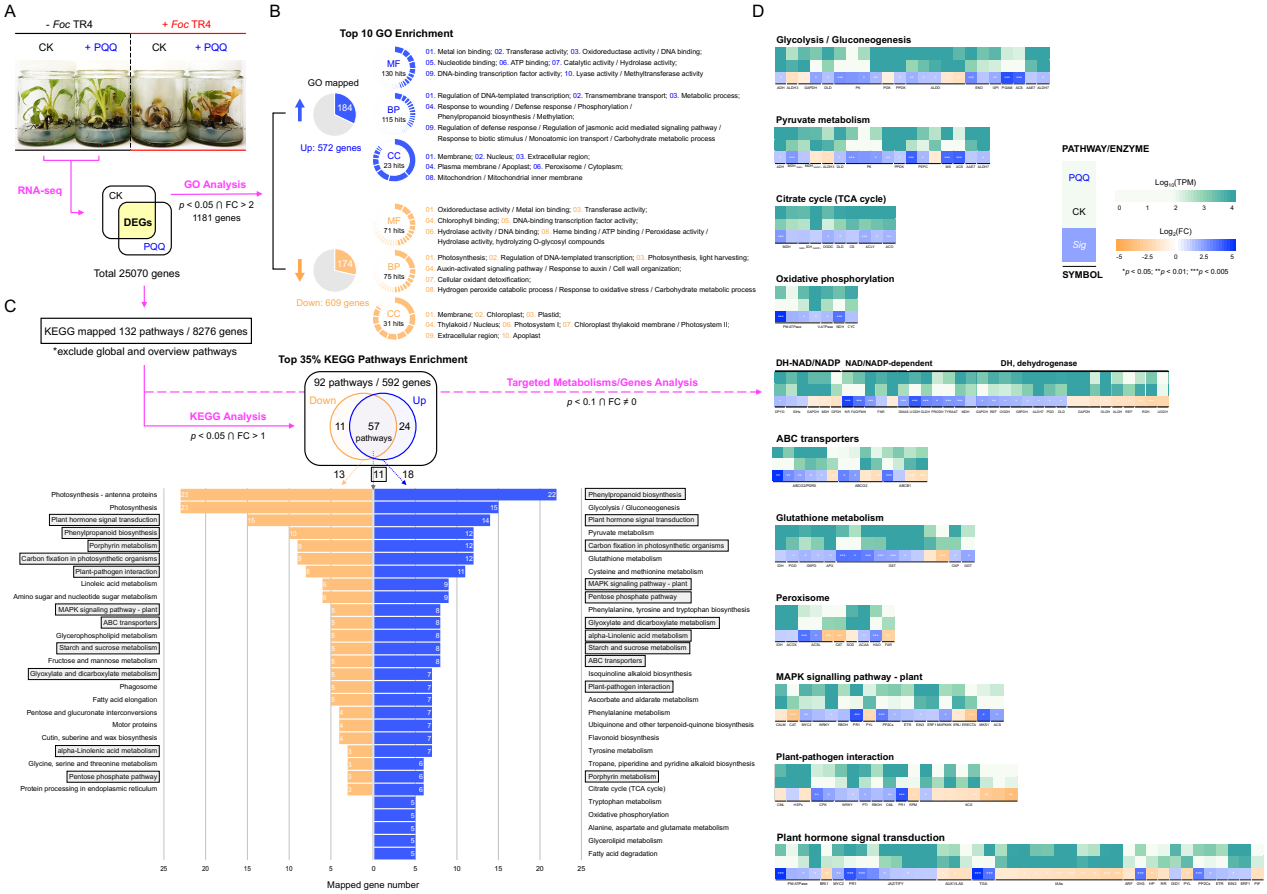

Fig. 4 Transcriptomic landscape of banana plants in response to PQQ. A Phenotypes of banana plant treated with 100 nM PQQ and infected by *Fusarium oxysporum* f. sp. cubense tropical race 4 (Foc TR4) at tissue culture growing stage. Total RNA was collected from these plants for the follow-up transcriptomic analysis. Differentially expressed genes (DEGs) defined by certain criteria were then subjected to **B** Gene Ontology (GO) terms enrichment analysis, **C** Kyoto Encyclopedia of Genes and Genomes (KEGG) pathways analysis and **D** targeted metabolisms and genes expression analysis. **B** The number inside the pie chart indicates the number of mapped GO terms, and the number inside the donut chart indicates the total hits of DEGs by the top 10 mapped GO terms presented orderly at the right of the donut chart. **C** The number inside the pie chart indicates the number of total DEGs-mapped KEGG pathways; the top 35% were labelled beside arrows linking to the column chart below; the number inside the column chart indicates the number of mapped DEGs; those mapped KEGG pathways shared by up- and down-regulated DEGs were marked by grey boxes. **D** Heatmaps showed the specific gene expression of targeted KEGG pathways. Details of gene symbols can be accessed in Table S7. The colour keys refer to the transcripts per kilobase million (TPM) and the corresponding fold changes (FC). Statistical significances between samples were indicated by asterisks (*p<0.05; **p<0.01; ***p<0.005); otherwise, not significant.

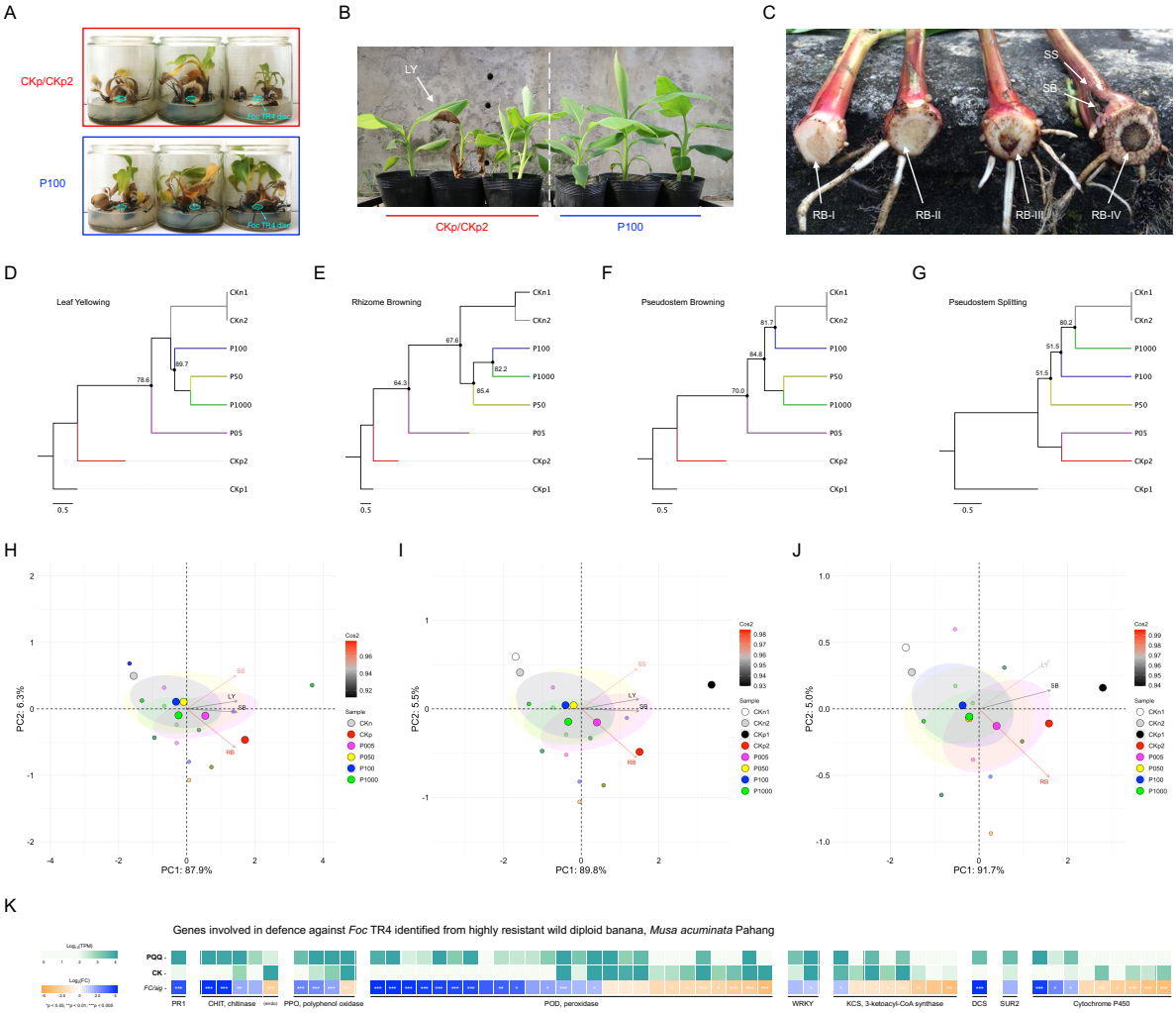

Fig. 5 PQQ contributes to the immunity of banana plants combating *Fusarium* wilt. Exogenous supplementation of PQQ contributes to the tolerance of banana plants against *Fusarium* oxysporum f. sp. cubense tropical race 4 (*Foc* TR4) in **A** tissue culture and in **B** soil conditions. *Foc* TR4 infection was performed through **A** discs (1.0 x 10^6 CFU/mL) placed at the centre of three replicates, highlighted by cyan dashed circles, or through **B** transplantation using infected soil (2.8 x 10^3 spore/gram). CKp/CKp2 and P100 are samples treated by ddH_2O and 100 nM PQQ, respectively. White arrows highlight four phenotypic indicators: **B** leaf yellowing (LY), **C** pseudostem splitting (SS), pseudostem (SB) and rhizome dark brown discolouration (RB) for the Panama disease resistance estimation; roman numerals suffixes of RB indicate the levels of disease severity from low to high as described in Materials and Methods. **D-F** Principal component analysis (PCA) on Panama disease indicators (LY, RB, SB and SS) of non-infected (CKn = CKn2; non-PQQ-pretreated) and Foc TR4-infected banana plants pretreated with different concentrations of PQQ; 0 mM (CKp = CKp2), 5 nM (P05), 50 nM (P50), 100 nM (P100) and 1000 nM (P1000); CKn1 and CKp1 are virtual negative and positive controls, respectively, included to assist the analyses; see Material and Methods for further details. Biplot vectors are the disease indicator loadings, whereas the position of each treatment is shown. Cos2 represents the quality of representation for variables on the factor map. **G-J** Unweighted pair group method with arithmetic mean (UPGMA) clustering dendrograms on Panama disease indicators of banana plants treated with different concentrations of PQQ; the dataset was accessed from **E** The trees were constructed based on the Euclidean distancing method with 1,000 multiscale bootstrap re-samplings; the approximately unbiased p-value of those internal nodes with < 90% were labelled. **K** Heatmaps showed the specific gene expression of genes involved in the immunity of wild bananas combating *Fusarium*. Details of gene symbols can be accessed in Table S8. The colour keys refer to the transcripts per kilobase million (TPM) and the corresponding fold changes (FC). Statistical significances between samples were indicated by asterisks (*p<0.05; **p<0.01; ***p<0.005); otherwise, not significant.

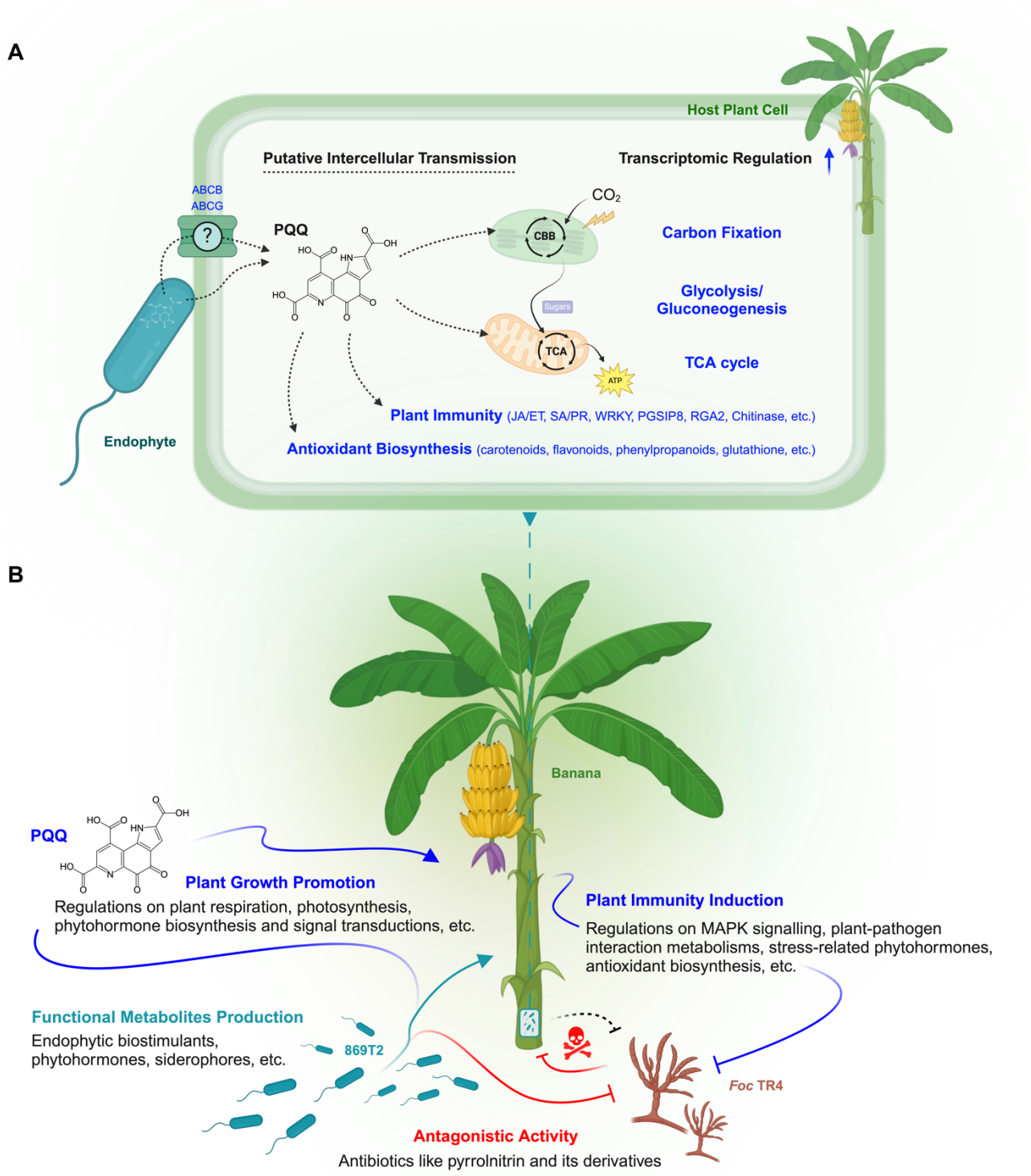

Fig. 6 Schematic illustration of plant-endophyte interactions that PQQ confers endophytic niches by coordinating host development. A Proposed PQQ molecular mechanisms in plant cells. Dashed lines indicate putative transmission from prokaryotic cells to or within eukaryotic cells. The mainly regulated genes and metabolisms identified with transcriptomics were highlighted in blue. **B** An overall viewpoint on how endophytes benefit the health of host plants and combat the *Fusarium* wilt of bananas. Icons were created with BioRender.com.